ELSEVIER

Atmospheric Environment 37 (2003) 4757–4768

ATMOSPHERIC ENVIRONMENT

www.elsevier.com/locate/atmosenv

Integrated approaches to modeling the organic and inorganic atmospheric aerosol components

Bonyoung Koo[a], Asif S. Ansari[b], Spyros N. Pandis[c,*]

[a] Department of Chemical Engineering, Carnegie Mellon University, Pittsburgh, PA 15213, USA
[b] Corporate Engineering Department, Bayer Corporation, Baytown, TX 77520, USA
[c] Department of Chemical Engineering and Engineering and Public Policy, Carnegie Mellon University, Pittsburgh, PA 15213, USA

Received 30 March 2003; accepted 9 August 2003

Abstract

A series of modeling approaches for the description of the dynamic behavior of secondary organic aerosol (SOA) components and their interactions with inorganics is presented. The models employ a lumped species approach based on available smog chamber studies and the UNIquac Functional-group Activity Coefficient (UNIFAC) method to estimate SOA water absorption. The additional water due to SOA species can change the partitioning behavior of the semi-volatile inorganics. Primary organic particles significantly influence the SOA partitioning between gas and aerosol phases. The SOA size distribution predicted by a bulk equilibrium approach is biased toward smaller sizes compared with that of a fully dynamic model. An improved weighting scheme for the bulk equilibrium approach is proposed in this work and is shown to minimize this discrepancy. SOA is predicted to increase the total aerosol water in Southern California by 2–13% depending on conditions. However, the effect of SOA water absorption on aerosol nitrate is insignificant for all the cases studied in Southern California.
© 2003 Elsevier Ltd. All rights reserved.

Keywords: Mathematical modeling; Secondary organic aerosol; Aerosol size distribution; Aerosol water content; UNIFAC

1. Introduction

Atmospheric aerosols consist of complex mixtures of inorganic and organic components (Pandis et al., 1995). The organic fraction of the aerosols generally contributes 30–60% of the total fine particulate matter (PM) in the atmosphere (Chow et al., 1994; Molnár et al., 1999), and thus has significant effects on atmospheric aerosol properties. While considerable progress has been made in understanding the physical and chemical properties of inorganic aerosols (Pilinis and Seinfeld, 1987; Wexler and Seinfeld, 1990, 1991; Kim et al., 1993a, b; Kim and Seinfeld, 1995; Jacobson et al., 1996; Nenes et al., 1998; Ansari and Pandis, 1999) our knowledge of organic aerosols remains limited due to their chemical complexity.

Organic carbon (OC) can be divided into two categories: primary and secondary OC. The former is emitted directly into the atmosphere and the latter is produced via photo-oxidation of hydrocarbon precursors. However, these two components cannot be identified directly. One of the approaches used for the estimation of the secondary organic aerosol (SOA) levels is use of chemical transport models. These mathematical models simulate the SOA precursor emission, organic aerosol formation, chemical transport, and deposition. The first modeling efforts treated each SOA component independently and neglected the interactions between organic and inorganic components (Pandis et al., 1992, 1993). In these approaches, the gas phase products of organic vapors condensed onto the aerosol phase when their gas phase concentrations exceeded their saturation

*Corresponding author. Fax: +1-412-268-7139.
E-mail address: spyros@andrew.cmu.edu (S.N. Pandis).

1352-2310/$ - see front matter © 2003 Elsevier Ltd. All rights reserved.
doi:10.1016/j.atmosenv.2003.08.016

concentrations. The second-generation models assumed that the SOA species form a solution. In this description, the SOA species can partition into the aerosol phase even if their gas phase concentrations are below their saturation levels (Pankow, 1994a, b). A series of studies have shown that a two-product absorption-model which assumes that each precursor produces two condensable products fits well the experimental data (Odum et al., 1996, 1997a, b; Hoffmann et al., 1997; Griffin et al., 1999a).

With the smog chamber results, Strader et al. (1999) simulated the SOA formation in a winter episode in southern California using a chemical transport model which assumes thermodynamic equilibrium between the gas and aerosol phases. A fully dynamic SOA model was developed by Bowman et al. (1997) and was applied to the simulation of smog chamber experiments. Meng et al. (1998) included an absorptive SOA model simulating two aromatic precursor groups in their three-dimensional aerosol model while their discussion focused on ozone and inorganic PM. Andersson-Sköld and Simpson (2001) employed the α-pinene chemical mechanism by Kamens et al. (1999) and a temperature-adjusted version of the Griffin et al. (1999b) model in a Lagrangian oxidant model and concluded that SOA formation from biogenic precursors is greater than that from anthropogenic ones in Nordic countries. Schell et al. (2001) drew a similar conclusion from their simulation of SOA formation over Europe. Griffin et al. (2002b) applied their three-dimensional atmospheric model which included the gas-phase chemical mechanism by Griffin et al. (2002a) and the thermodynamic module by Pun et al. (2002) to a summer smog episode in southern California and showed that anthropogenic sources are dominant contributors to total SOA formation in the area. Those three-dimensional models generally employ the equilibrium approach to reduce the computational costs. However, the ability of the equilibrium approach to simulate accurately the total SOA concentration and its size distribution has not been evaluated.

The contribution of SOA to the total aerosol water content has been another important issue. Organic components may affect the hygroscopic properties of atmospheric aerosols (Zhang et al., 1993; Saxena et al., 1995; Cruz and Pandis, 1998, 2000). Predicting the water absorption by the organic fraction of atmospheric aerosols is challenging because thermodynamic data such as water activity coefficients are scarce for atmospherically relevant organic compounds. Recent attempts to estimate the hygroscopic properties of SOA species include the use of group contribution methods (Saxena and Hildemann, 1997; Jang and Kamens, 1998; Ansari and Pandis, 2000; Cocker et al., 2001; Hemming and Seinfeld, 2001; Peng et al., 2001; Seinfeld et al., 2001). The main advantage of this approach is that the interaction between numerous organic species can be reduced to that of a small number of functional groups. Although a few efforts to predict the thermodynamics of a mixture of both organics and inorganics have recently been reported (Clegg et al., 2001; Ming and Russell, 2002), they are still limited due to the paucity of thermodynamic data for species of atmospheric interest.

In spite of all the efforts there are still remaining questions: (a) which of the equilibrium and dynamic approaches should be used to model organic aerosols? (b) how does water absorption by SOA affect the partitioning of inorganics between gas and aerosol phases? To address these issues, in this study the equilibrium and fully dynamic SOA models are integrated with available inorganic models and evaluated against ambient atmospheric data. A two-product absorption-model for SOA is coupled with an inorganic aerosol model in a one-dimensional chemical transport model. The equilibrium and fully dynamic behavior of SOA components coupled with that of inorganic components is then discussed.

2. SOA modeling

The host model is a one-dimensional Lagrangian trajectory model which simulates gas-phase chemistry, vertical dispersion, dry deposition, and primary emissions (Pandis et al., 1992). The SAPRC gas-phase chemical mechanism has been extended to include formation of organic precursors (Carter, 1990; Pandis et al., 1992). Included in this framework are equilibrium and dynamic inorganic aerosol modules. In the equilibrium approach, a thermodynamic inorganic model, ISORROPIA by Nenes et al. (1998) determines the bulk inorganic mass to be transferred between gas and aerosol phases and a weighting scheme based on the surface area (Pandis et al., 1993) distributes it over the aerosol size distribution. On the other hand, the multicomponent aerosol dynamic model (MADM) by Pilinis et al. (2000) is used to simulate the fully dynamic behavior of inorganics. The moving size distribution used internally in the aerosol modules is mapped onto a fixed grid system by a linear interpolation scheme for mixing between different computational cells. The inorganic model is described in detail in Koo et al. (2003).

The equilibrium and fully dynamic SOA models were incorporated into this framework. In the dynamic approach, a fundamental flux equation determines the mass transfer rates of organic species for each size section, which are proportional to the difference between their bulk gas-phase concentrations and equilibrium concentrations at the particle surface (Seinfeld

and Pandis, 1998):

$$J_{i,k} = 2\pi N_k d_k D_i f(Kn, a)(c_i - c_i^{eq}\eta),$$

where $J_{i,k}$ is the flux of species i to aerosol size section k, N_k and d_k are the number and mean diameter of particles in the section k, respectively, D_i, c_i, and c_i^{eq} is the diffusivity, bulk gas-phase concentration, and equilibrium concentration at the particle surface of species i, respectively, $f(Kn, a)$ is the correction for non-continuum effects and imperfect accommodation, Kn is the Knudsen number, a is the accommodation coefficient, and η is the Kelvin effect correction. The equilibrium concentration of each species is given by assuming absorptive partitioning in a pseudo-ideal solution:

$$c_i^{eq} = x_{i,k} c_i^*,$$

where $x_{i,k}$ is the mole fraction of species i in the section k, c_i^* is the effective saturation concentration of species i (it accounts for non-ideality of the solution).

The equilibrium approach employs the secondary organic aerosol model (SOAM II) by Strader et al. (1999). In this model, the bulk equilibrium gas and aerosol concentrations are first calculated. Considering partitioning of n condensable products formed via photo-oxidation of hydrocarbon precursors between gas and aerosol phases:

$$c_{t,i} = c_{g,i} + c_{a,i} = \alpha_i \Delta HC_i,$$

where $c_{t,i}$, $c_{g,i}$, and $c_{a,i}$ are the total, gas-phase, and aerosol-phase concentrations of product i in $\mu g\,m^{-3}$, respectively, ΔHC_i is the corresponding amount of reacted hydrocarbon precursor in $\mu g\,m^{-3}$, and α_i is the stoichiometric coefficient for product i (in most smog chamber experiments α is represented on mass basis, not molar basis). Assuming the pseudo-ideal solution, a set of n nonlinear equations

$$c_{a,i} = c_{t,i} - x_i c_i^* \quad \text{for } i = 1, n,$$

$$x_i = \frac{c_{a,i}/M_i}{c_0/M_0 + \sum_{j=1}^{n} c_{a,j}/M_j}$$

is obtained where x_i is the mole fraction of product i in the absorbing organic phase, M_i is the molecular weight of product i, and c_0 and M_0 are the concentration and molecular weight of pre-existing organic material in the absorbing phase, respectively. Solving this equation set yields the bulk aerosol composition at equilibrium. The aerosol size distribution is then determined by distributing the change in aerosol mass during the time step into each size bin using a weighting factor (Pandis et al., 1993). The fraction, $f_{i,k}$, of total flux of species i between gas and aerosol phases that condenses onto or evaporates from an aerosol size section k is given by

$$f_{i,k} = \frac{2\pi N_k d_k D_i (c_i - c_i^{eq})/(\beta_k + 1)}{\sum_k 2\pi N_k d_k D_i (c_i - c_i^{eq})/(\beta_k + 1)}$$

where $\beta_k = 2\lambda/ad_k$ and λ is the mean free path of air (Pandis et al., 1993). Assuming that c_i^{eq} is independent of particle size, the fraction is reduced to

$$f_{i,k} = \frac{N_k d_k/(\beta_k + 1)}{\sum_k N_k d_k/(\beta_k + 1)} = f_k$$

which is the weighting factor based on the surface area used by Pandis et al. (1993). In general, however, c_i^{eq} depends on the chemical composition of the particle. With the pseudo-ideal solution assumption

$$f_{i,k} = \frac{N_k d_k (c_i - x_{i,k} c_i^*)/(\beta_k + 1)}{\sum_k N_k d_k (c_i - x_{i,k} c_i^*)/(\beta_k + 1)}.$$

Since the fraction determines the composition of each size section the above equation should be solved iteratively at each time step. Assuming that the chemical composition changes slowly during a time step (a few minutes), however, the mole fractions can be approximated with those from the previous time step.

In the original SOAM II three lumped aromatics and toluene are included in the group of species that are assumed to produce two condensable products (these species will be referred as two-product precursors henceforth). The original model was updated based on the smog chamber experiments by Griffin et al. (1999a) with the addition of two biogenic olefins (α-pinene and β-pinene) to the two-product precursors. For the remaining species only one product was assumed due to the lack of experimental data (these species will be referred as one-product precursors henceforth). However, the saturation concentrations estimated for the products of one-product precursors in SOAM II are uncertain. Tao and McMurry (1989) measured vapor pressures for glutaric acid and adipic acid. Their values extrapolated to 281.5 K were 5 and $0.06\,\mu g\,m^{-3}$, respectively. Bilde and Pandis (2001) and Bilde et al. (2003) measured vapor pressures of C3–C9 dicarboxylic acids and their values extrapolated to 281.5 K ranged from 0.001 to $9\,\mu g\,m^{-3}$. These species have been suggested as secondary products from photo-oxidation of biogenic and anthropogenic olefins (Grosjean and Friedlander, 1980; Yokouchi and Ambe, 1986; Stephanou and Stratigakis, 1993). Estimated values for SOA products from olefins in SOAM II were quite low ranging from 0.004 to $0.008\,\mu g\,m^{-3}$ (Strader et al., 1999). Since the estimates by Strader et al. (1999) appear to be the lower bound of the measured values, the saturation concentrations for one-product precursors were increased by two orders of magnitude in this model. Model species and their parameters are listed in Table 1 and are discussed in more detail in Pandis et al. (1992). Model sensitivity to these parameters will be discussed in a subsequent section.

The temperature dependence of saturation concentrations is considered by the Clausius–Clapeyron

Table 1
Model species[a] and parameters

Precursors[b]	Aerosol species[b]	α ($\mu g\,m^{-3}$ $(\mu g\,m^{-3})^{-1}$)	c^* ($\mu g\,m^{-3}$)[c]
One-product precursors			
AAR1	AEA1	0	—
AAR2	AEA2	0[d]	—
AAR3	AEA3	0.004[d]	2.36[e]
AAR4	AEA4	0.014[d]	3.14[e]
OLE1	AEO1	0.002	1.57[e]
OLE2	AEO2	0	—
OLE3	AEO3	0.004	1.96[e]
C7OL	AEC7	0.013	2.36[e]
C8OL	AEC8	0.035	2.75[e]
C9OL	AEC9	0.044	2.75[e]
BALD	AEBA	0.0008	2.75[e]
PBZN	AEPB	0.0005	3.93[e]
PHEN	AEPH	0.031	2.36[e]
CRES	AECR	0.034	2.75[e]
NPHE	AENP	0.037	3.14[e]
Two-product precursors			
AAR5	AEA5	0.071	18.87
	AEX5	0.138	526.3
AAR6	AEA6	0.038	23.81
	AEX6	0.167	714.3
AAR7	AEA7	0.038	23.81
	AEX7	0.167	714.3
TOLU	AETL	0.071	18.87
	AETM	0.138	526.3
APIN	AEAP	0.038	5.848
	AEAQ	0.326	250.0
BPIN	AEBP	0.130	22.73
	AEBQ	0.406	204.1

[a] Organic species only.
[b] For actual species refer to Carter (1990) and Pandis et al. (1992).
[c] Reference temperature is 313 K.
[d] Corrected with original reference values (Grosjean and Seinfeld, 1989).
[e] Values from Strader et al. (1999) multiplied by 100 (see text).

equation

$$c_i^* = c_{i,0}^* \frac{T_0}{T} \exp\left[\frac{\Delta H}{R}\left(\frac{1}{T_0} - \frac{1}{T}\right)\right],$$

where c_i^* and $c_{i,0}^*$ are the saturation concentrations at temperature T and T_0, respectively, R is the gas constant, and ΔH is the enthalpy of vaporization. While the reported values for ΔH vary from species to species we assume an average value of 17.5 kcal mol^{-1} for all species (Sheehan and Bowman, 2001).

Recent studies have shown that primary OC can often form a solution with SOA species and thus act like pre-existing organic phase (Lee and Kamens, 2002). In this work primary organic mass is regarded as pre-existing absorbing material. The sensitivity to this assumption will be explored in a later section.

3. SOA water absorption

To determine the contribution of SOA to the total aerosol water content and its effect on the partitioning of semi-volatile inorganic components between gas and aerosol phases, the coupled approach by Ansari and Pandis (2000) was employed. In this approach the SOA water absorption is determined via available group contribution methods and then used as an additional input in the calculation of inorganic aerosol composition with a thermodynamic model. In this work, the amount of water absorbed by SOA species calculated by UNIFAC is added to the water content associated with inorganics from the ZSR relationship (Stokes and Robinson, 1966) and this total water is then used to calculate the equilibrium concentrations for inorganics in ISORROPIA.

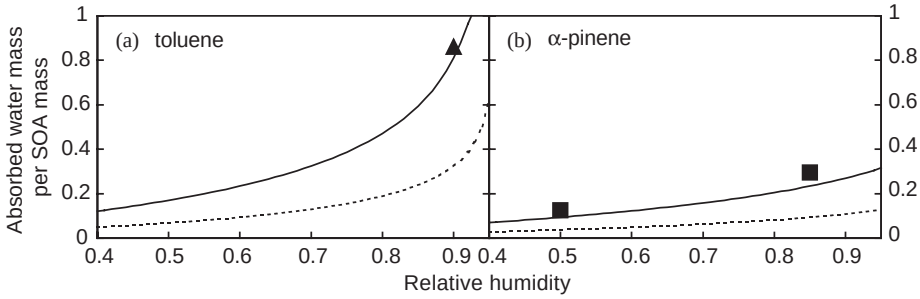

Fig. 1. SOA water absorption measured from oxidation products of toluene (Petäjä et al., 2002; triangle) and α-pinene (Cocker et al., 2001; square) and predicted by the corrected (solid line) and original (dashed line) UNIFAC using corresponding representative species.

Table 2
Selected representative SOA species

Precursor group	Representative SOA species
Alkanes	Nonanoic acid and pentadecanoic acid[a]
Anthropogenic olefins	Hydroxyglutaric acid and hydroxyadipic acid[b]
Biogenic olefins	Pinic acid and norpinonic acid[c]
Aromatics	Methyl maleic anhydride[d]
	Dinitrocresol[e]
	Nitrophenol[f]

[a] Assumed (refer to the text).
[b] From oxidation of cyclohexene with ozone (Kalberer et al., 2000).
[c] From oxidation of α- and β-pinene with ozone (Yu et al., 1999).
[d] From oxidation of *m*- and *p*-xylene, 1,2,4-trimethylbenzene, and toluene with NO_x (Forstner et al., 1997).
[e] From oxidation of *o*-cresol with NO_x (Grosjean, 1985).
[f] From oxidation of phenol with OH and NO_3 (Atkinson et al., 1992).

Since the chemical identity of most SOA products is unknown, it is assumed that a set of major identified SOA species can be used to represent the hygroscopic properties of the actual SOA mixtures. Table 2 presents selected representative SOA products for each hydrocarbon precursor group. Since there are few studies of SOA products from alkane precursors we used the corresponding monocarboxylic acids from nonane and pentadecane as the representative species.

Since UNIFAC was originally developed for chemical separation processes where chemical species of most interest are short-chain monofunctional compounds, its estimates for the properties of multifunctional compounds which are common in the atmosphere can be highly uncertain. It has been reported that UNIFAC tends to overpredict water activities for some SOA species, which results in underprediction of water content (Ansari and Pandis, 2000). Moreover, the use of representative SOA species can increase this uncertainty. Fig. 1 shows that the difference between measurements using actual SOA and UNIFAC estimation can be as high as a factor of 2–3. For the base case simulation we corrected the UNIFAC estimation by multiplying by a factor of 2.5, at least bringing the results in good agreement with the few available measurements.

4. Results and discussion

4.1. Base case simulation

Both the equilibrium and dynamic models described above were applied to an air pollution episode on 28 August 1987 in southern California during the Southern California Air Quality Study (SCAQS). The episode has been studied by a variety of groups (Pandis et al., 1992, 1993; Jacobson, 1997; Meng et al., 1998; Kleeman and Cass, 1998) and details can be found in Koo et al. (2003). Twenty-four simulations, one trajectory for each hour, were performed. The predicted contributions of the main precursor groups to the predicted 24-h average total SOA mass are shown in Table 3. Aromatic precursors account for about three quarters of the total SOA mass produced, a result consistent with the estimates of Grosjean and Seinfeld (1989) and Pandis et al. (1992) for this episode. Fig. 2 shows total OC (primary OC and SOA) concentrations in $PM_{2.5}$ predicted by the equilibrium and dynamic models. Both models underpredict fine OC concentrations compared with the measurements by Turpin and Huntzicker (1991). The discrepancy in the morning period appears mainly due to underestimation of primary emission which is the main source of organic aerosol in these hours. It has been estimated, however, that in the afternoon of this day, a significant fraction of the organic aerosol is secondary (Fig. 3). The peak SOA mass is predicted at 17:00 PST when SOA concentration

Table 3
Predicted contribution of hydrocarbon precursors to 24-h average total SOA concentration at Claremont on 28 August 1987

Precursors	SOA concentration ($\mu g\,m^{-3}$)	Contribution to total SOA (%)
Alkanes	0.33	12
Anthropogenic olefins	0.30	10
Biogenic olefins	0.07	3
Aromatics	2.2	75
Total	2.9	100

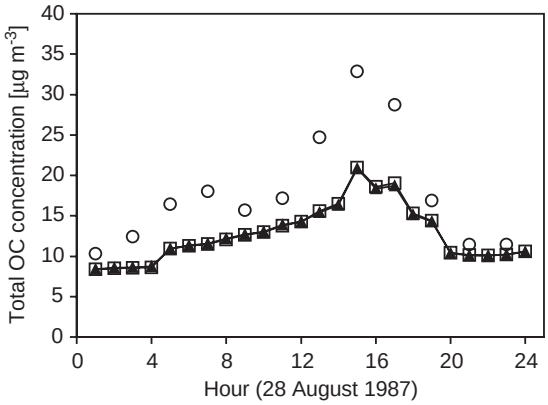

Fig. 2. Total OC concentrations in $PM_{2.5}$ predicted by the equilibrium (solid line with squares) and dynamic (solid line with triangles) models; circles represent the measured OC by Turpin and Huntzicker (1991).

and the ratio of SOA to total organic mass in $PM_{2.5}$ are $4.7\,\mu g\,m^{-3}$ and 25%, respectively. These values are smaller than the $15.7\,\mu g\,m^{-3}$ (assuming 0.7 g of carbon per gram organic aerosol) estimated by Turpin and Huntzicker (1991) resulting in underprediction of OC concentration for this period. The peak hour agrees with their estimate. Except during the period between 14:00 and 18:00 PST, the model predictions agree with the estimates of Turpin and Huntzicker (1991) within their uncertainty range. The underprediction of SOA can be the result of an overestimation of saturation vapor pressures. This possibility will be discussed in the model sensitivity section. It should also be noted that there exist significant uncertainties in the hydrocarbon emission inventory used in this model (Pandis et al., 1992).

SOA concentrations in $PM_{2.5}$ (PM with diameter $\leqslant 2.5\,\mu m$) and PM_{10} (PM with diameter $\leqslant 10\,\mu m$) predicted by the equilibrium model with the modified and old weighting schemes and dynamic model are compared in Fig. 4. Although PM_{10} SOA concentrations predicted by all three models are in agreement, the

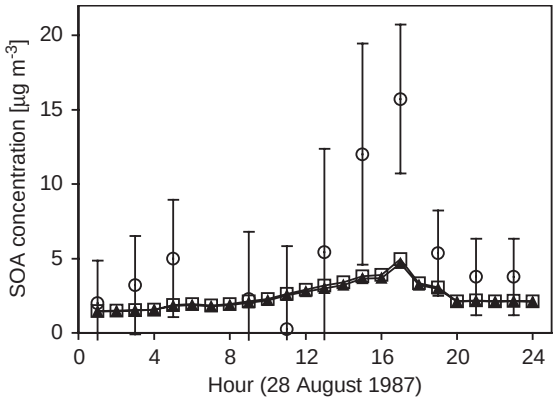

Fig. 3. $PM_{2.5}$ SOA concentrations predicted by the equilibrium (solid line with squares) and dynamic (solid line with triangles) models; circles with error bars represent the estimated SOA by Turpin and Huntzicker (1991).

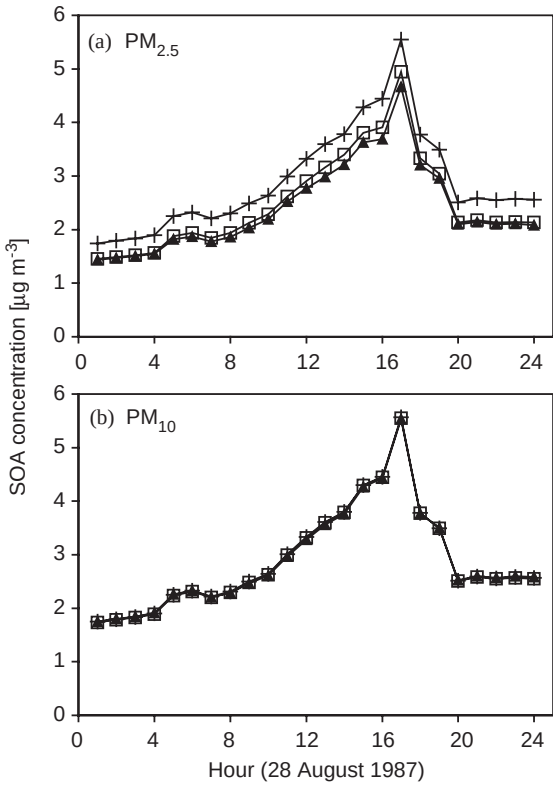

Fig. 4. SOA concentrations predicted by the equilibrium model with the modified (solid line with squares) and old (solid line with crosses) weighting schemes and dynamic model (solid line with triangles).

equilibrium model with the old weighting scheme overpredicts $PM_{2.5}$ SOA mass by 21% on average (and underpredicts the SOA in the coarse fraction). Predicted

SOA size distributions clearly show that the equilibrium model with the modified weighting scheme gives better agreement with the dynamic model than that with the old weighting scheme (Fig. 5).

The effect of SOA water absorption in the base case was quantified by repeating the simulation neglecting the SOA contribution to water. Fig. 6 shows that total aerosol water concentrations predicted by both models increase by about 5% due to SOA components. The changes in aerosol nitrate are <1%. Diurnal variations of the increases are shown in Fig. 7. Although SOA absorbs more water at night due to higher relative humidity the increase in aerosol water is also enhanced in the afternoon due to the higher SOA concentration. Both models agree well except during the period of 1:00–3:00 and 15:00–17:00 PST when the dynamic model predicts a larger increase in aerosol water content. This discrepancy seems to be related to the different inorganic composition predicted by the two models. Since total aerosol water content is determined by ISORROPIA using inorganics as well as water absorbed by SOA, the equilibrium and dynamic model can give different predictions if SOA water absorption affects inorganics differently in each model. Indeed, it is seen that the changes in nitrate predicted by the two models deviate during the same periods as those in aerosol water (Fig. 7).

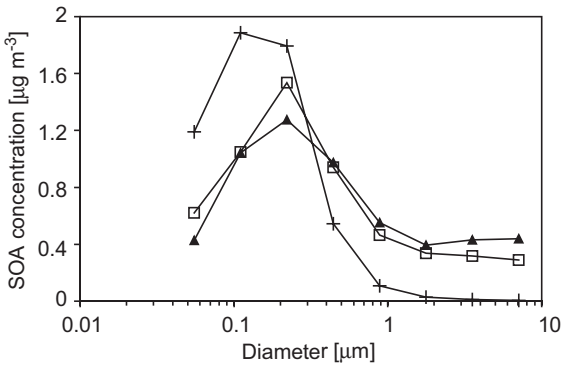

Fig. 5. SOA size distributions predicted by the equilibrium model with the modified (solid line with squares) and old (solid line with crosses) weighting schemes and dynamic model (solid line with triangles) at 17:00 PST.

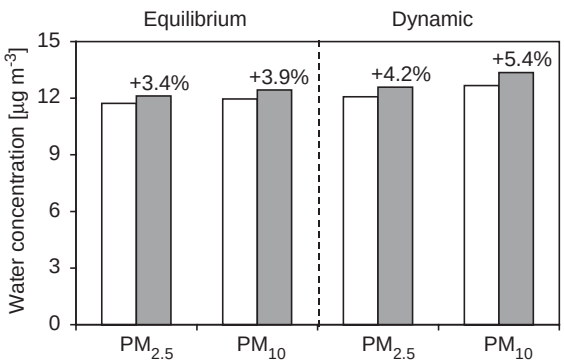

Fig. 6. Changes in 24-h average aerosol water content due to SOA components predicted by the equilibrium and dynamic models; blank and filled bars represent model results without and with SOA water absorption, respectively.

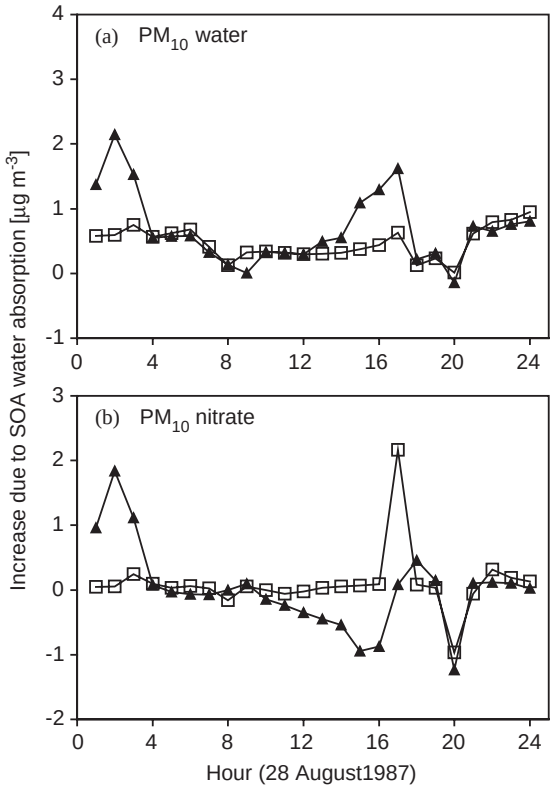

Fig. 7. Increases in water and nitrate due to SOA water absorption predicted by the equilibrium (solid line with squares) and dynamic model (solid line with triangles).

4.2. Sensitivity to saturation concentrations

Three tests were performed to investigate the sensitivity of the results to the saturation concentration values used. In the first case, the saturation concentrations for one-product precursors were reduced by 2 orders of magnitude, that is the values used by Strader et al. (1999), for the simulation of a winter episode in central California. In the second case, the saturation concentrations for all precursors were reduced by a factor of 10. The third case uses a fixed equilibrium gas concentration of 2 ppt for all SOA products, which can be viewed as an upper limit estimate on the formation of SOA (Pandis et al., 1992). Recently, Jang et al. (2002)

reported that in the presence of inorganic acids organic carbonyls formed via photo-oxidation could react heterogeneously to produce low vapor pressure products resulting in higher SOA yields. A scenario where the SOA species form a solution that does not include the primary OC was also tested.

Table 4 shows predicted daily average SOA concentrations in $PM_{2.5}$ and PM_{10} for the various scenarios. Reducing the saturation concentrations for one-product precursors resulted in only slight increases in the predicted SOA mass mainly because the contributions from one-product precursors to SOA are minor. Reducing the saturation concentrations for all precursors by a factor of 10 increased the predicted SOA mass more than twice. In the case with the fixed low equilibrium gas concentration the total concentration of SOA produced goes up to $9\,\mu g\,m^{-3}$, which accounts for about 40% of total organic aerosol mass. Finally the inclusion of primary OC as an absorbing material has a significant effect on the model results. Without pre-existing organic mass the predicted SOA concentration decreased to $1\,\mu g\,m^{-3}$. Model predictions of SOA mass in $PM_{2.5}$ and PM_{10} by the equilibrium model with the modified weighting scheme are in good agreement with those of the dynamic model in all scenarios.

Increases in 24-h average aerosol water content due to SOA components are presented in Table 5. The responses are similar to those of daily average SOA mass. Reducing the saturation concentrations for all precursors almost doubles the SOA contribution to daily average aerosol water while reducing those for one-product precursors only has little effect. Maximum SOA formation leads to 13% increase in daily average aerosol water content. In the case with no pre-existing absorbing material water absorbed by SOA species is insignificant. The differences in 24-h average aerosol nitrate due to SOA water absorption are $<3\%$ for all cases.

4.3. Sensitivity to UNIFAC estimations

To test uncertainty in UNIFAC estimations we repeated the base case simulations with doubled SOA water absorption and the original UNIFAC estimation (approximately half). The model predictions of SOA water absorption are presented in Table 6. As expected the amount of water absorbed by SOA increases or decreases almost proportionally. The changes of aerosol nitrate are negligible in all cases and not linearly related with SOA water absorption.

Table 4
Sensitivity analysis of 24-hr average SOA concentrations predicted by the equilibrium and dynamic models

Case	Total SOA concentration ($\mu g\,m^{-3}$)			
	$PM_{2.5}$		PM_{10}	
	Equilibrium	Dynamic	Equilibrium	Dynamic
Base case	2.5 (20%)[a]	2.4 (19%)	2.9 (17%)	2.9 (17%)
c^* for one-product precursors $\times$ 0.01	2.7 (21%)	2.6 (20%)	3.0 (17%)	3.0 (17%)
c^* for all precursors $\times$ 0.1	5.5 (35%)	5.3 (34%)	6.1 (30%)	6.1 (30%)
c^{eq} for all species $=2$ ppt	9.1 (47%)	9.0 (47%)	9.1 (39%)	9.1 (39%)
No c_0	0.96 (8.6%)	1.0 (9.0%)	0.96 (6.3%)	1.0 (6.7%)

[a] The numbers in parentheses are SOA fractions of total organic mass.

Table 5
Contributions of SOA components to 24-h average aerosol water content predicted by the equilibrium and dynamic models

Case	Increase in total aerosol water due to SOA ($\mu g\,m^{-3}$)			
	$PM_{2.5}$		PM_{10}	
	Equilibrium	Dynamic	Equilibrium	Dynamic
Base case	0.40 (3.4%)[a]	0.51 (4.2%)	0.47 (3.9%)	0.69 (5.4%)
c^* for one-product precursors $\times$ 0.01	0.42 (3.6%)	0.41 (3.4%)	0.48 (4.0%)	0.56 (4.4%)
c^* for all precursors $\times$ 0.1	0.92 (7.9%)	0.82 (6.8%)	1.0 (8.6%)	1.1 (8.5%)
c^{eq} for all species $=2$ ppt	1.5 (13%)	1.7 (14%)	1.5 (13%)	1.7 (13%)
No c_0	0.18 (1.6%)	0.29 (2.4%)	0.18 (1.5%)	0.27 (2.1%)

[a] The numbers in parentheses are percent increases.

Table 6
Increases in 24-h average total (PM_{10}) aerosol water due to SOA components predicted by the equilibrium and dynamic model

Case	Increase in water due to SOA components ($\mu g\,m^{-3}$)	
	Equilibrium	Dynamic
SOA water absorption × 2	0.97 (8.1%)[a]	0.99 (7.8%)
Original UNIFAC estimation	0.21 (1.7%)	0.29 (2.3%)

[a] The numbers in parentheses are percent increases.

4.4. Kelvin effect

In our aerosol model the Kelvin effect is neglected since the lower limit of the particle size distribution used is 0.04 μm. To quantify the Kelvin effect on the SOA size distribution we repeated the base case simulation with the Kelvin effect correction. The correction factor, $\eta_{i,k}$, for species i in an aerosol size section k can be expressed as

$$\eta_{i,k} = \exp\left(\frac{4\sigma_i M_i}{RT\rho d_k}\right),$$

where σ_i is surface tension of species i and ρ is particle-phase density (Seinfeld and Pandis, 1998). Average surface tension of 80 dyne cm^{-1} was used for electrolytes in aqueous solution (Li et al., 1999) and 30 dyne cm^{-1} for organic species (Nath, 1999). The model results confirmed that the Kelvin effect correc tion makes negligible difference in the SOA size distribution.

5. Conclusions

A mathematical model which simulates the equilibrium and fully dynamic behavior of both SOA and inorganic aerosols was implemented in a one-dimensional chemical transport model. The simulation based on a summer episode in southern California shows that 17% of total organic mass comes from the secondary products and among hydrocarbon precursors the aromatic group is the largest contributor. While primary OC is treated in the same way in both equilibrium and dynamic models, discrepancies between the SOA predictions by the two models become more significant when primary OC is assumed to form a solution with SOA species because the inclusion of primary OC leads to higher SOA predictions. Predicted SOA mass by the equilibrium model with the modified weighting scheme to consider composition-dependent equilibrium concentrations gave excellent agreement with that of the dynamic model. Using the approach of Ansari and Pandis (2000) to characterize water absorption of SOA species, the contribution of SOA to aerosol water content and its possible effect on the partitioning of aerosol nitrate were simulated. Increases in daily average aerosol water due to SOA components are about 5% for the base case and 13% for the maximum SOA formation case. With SOA water absorption multiplied by 2, this increase goes up to 8% for the base case. The original UNIFAC estimation predicted only 2% of increase in aerosol water. Model predictions of nitrate partitioning are little affected by the model treatment of the SOA species. The changes in aerosol nitrate are $<3\%$ in all the scenarios studied in this work. It should be noted, however, the method used in this work to couple SOA and inorganics suffers from the same weaknesses as those described by Ansari and Pandis (2000).

Based on the simulations conducted in this work, the equilibrium model with the modified weighting scheme is good enough to simulate the dynamic behavior of SOA in the atmosphere. This approach is well suited for computationally intensive three-dimensional air quality models. UNIFAC provides an initial approximation of SOA water absorption, which can account for significant fraction of total aerosol water content depending on the atmospheric conditions, while our understanding of the chemical properties of the SOA species is still limited. However, the interaction between organic and inorganic aerosol components through aerosol water content had only a minor effect on nitrate partitioning between gas and aerosol phases.

Acknowledgements

This work was funded by the National Science Foundation and the EPA STAR grant R 826371.

References

Andersson-Sköld, Y., Simpson, D., 2001. Secondary organic aerosol formation in northern Europe: a model study. Journal of Geophysical Research 106, 7357–7374.

Ansari, A.S., Pandis, S.N., 1999. Prediction of multicomponent inorganic atmospheric aerosol behavior. Atmospheric Environment 33, 745–757.

Ansari, A.S., Pandis, S.N., 2000. Water absorption by secondary organic aerosol and its effect on inorganic aerosol behavior. Environmental Science and Technology 34, 71–77.

Atkinson, R., Aschmann, S.M., Arey, J., 1992. Reactions of OH and NO_3 radicals with phenol, cresols, and 2-nitrophenol at 296 ± 2 K. Environmental Science and Technology 26, 1397–1403.

Bilde, M., Pandis, S.N., 2001. Evaporation rates and vapor pressures of individual aerosol species formed in the atmospheric oxidation of α- and β-pinene. Environmental Science and Technology 35, 3344–3349.

Bilde, M., Svenningsson, B., Mønster, J., Rosenørn, T., 2003. Even–odd alternation of evaporation rates and vapor pressures of C3–C9 dicarboxylic acid aerosols. Environmental Science and Technology 37, 1371–1378.

Bowman, F.M., Odum, J.R., Seinfeld, J.H., Pandis, S.N., 1997. Mathematical model for gas-particle partitioning of secondary organic aerosols. Atmospheric Environment 31, 3921–3931.

Carter, W.P.L., 1990. A detailed mechanism for the gas-phase atmospheric reactions of organic compounds. Atmospheric Environment 24A, 481–518.

Chow, J.C., Watson, J.G., Fujita, E.M., Lu, Z., Lawson, D.R., Ashbaugh, L.L., 1994. Temporal and spatial variations of $PM_{2.5}$ and PM_{10} aerosol in the Southern California air-quality study. Atmospheric Environment 28, 2061–2080.

Clegg, S.L., Seinfeld, J.H., Brimblecombe, P., 2001. Thermodynamic modelling of aqueous aerosols containing electrolytes and dissolved organic compounds. Journal of Aerosol Science 32, 713–738.

Cocker, D.R., Clegg, S.L., Flagan, R.C., Seinfeld, J.H., 2001. The effect of water on gas-particle partitioning of secondary organic aerosol, Part I: α-pinene/ozone system. Atmospheric Environment 35, 6049–6072.

Cruz, C.N., Pandis, S.N., 1998. The effect of organic coatings on the cloud condensation nuclei activation of inorganic atmospheric aerosol. Journal of Geophysical Research 103, 13111–13123.

Cruz, C.N., Pandis, S.N., 2000. Deliquescence and hygroscopic growth of mixed inorganic–organic atmospheric aerosol. Environmental Science and Technology 34, 4313–4319.

Forstner, H.J.L., Flagan, R.C., Seinfeld, J.H., 1997. Secondary organic aerosol from the photooxidation of aromatic hydrocarbons: molecular composition. Environmental Science and Technology 31, 1345–1358.

Griffin, R.J., Cocker, D.R., Flagan, R.C., Seinfeld, J.H., 1999a. Organic aerosol formation from the oxidation of biogenic hydrocarbons. Journal of Geophysical Research 104, 3555–3567.

Griffin, R.J., Cocker, D.R., Seinfeld, J.H., Dabdub, D., 1999b. Estimate of global atmospheric organic aerosol from oxidation of biogenic hydrocarbons. Geophysical Research Letters 26, 2721–2724.

Griffin, R.J., Dabdub, D., Seinfeld, J.H., 2002a. Secondary organic aerosol, 1, Atmospheric chemical mechanism for production of molecular constituents. Journal of Geophysical Research 107, 4332, doi:10.1029/2001JD000541.

Griffin, R.J., Dabdub, D., Kleeman, M.J., Fraser, M.P., Cass, G.R., Seinfeld, J.H., 2002b. Secondary organic aerosol, 3, Urban/regional scale model of size- and composition-resolved aerosols. Journal of Geophysical Research 107, 4334, doi:10.1029/2001JD000544.

Grosjean, D., 1985. Reactions of *o*-cresol and nitrocresol with NO_x in sunlight and with ozone-nitrogen dioxide mixtures in the dark. Environmental Science and Technology 19, 968–974.

Grosjean, D., Friedlander, S.K., 1980. Formation of organic aerosols from cyclic olefins and diolefins. In: Hidy, G.M. (Ed.), The Character and Origins of smog Aerosols. Wiley, New York, pp. 435–473.

Grosjean, D., Seinfeld, J.H., 1989. Parameterization of the formation potential of secondary organic aerosols. Atmospheric Environment 23, 1733–1747.

Hemming, B.L., Seinfeld, J.H., 2001. On the hygroscopic behavior of atmospheric organic aerosols. Industrial and Engineering Chemistry Research 40, 4162–4171.

Hoffmann, T., Odum, J.R., Bowman, F., Collins, D., Klockow, D., Flagan, R.C., Seinfeld, J.H., 1997. Formation of organic aerosols from the oxidation of biogenic hydrocarbons. Journal of Atmospheric Chemistry 26, 189–222.

Jacobson, M.Z., 1997. Development and application of a new air pollution modeling system—Part III. Aerosol-phase simulations. Atmospheric Environment 31, 587–608.

Jacobson, M.Z., Tabazadeh, A., Turco, R.P., 1996. Simulating equilibrium within aerosols and nonequilibrium between gases and aerosols. Journal of Geophysical Research 101, 9079–9091.

Jang, M., Kamens, R.M., 1998. A thermodynamic approach for modeling partitioning of semivolatile organic compounds on atmospheric particulate matter: humidity effects. Environmental Science and Technology 32, 1237–1243.

Jang, M., Czoschke, N.M., Lee, S., Kamens, R.M., 2002. Heterogeneous atmospheric aerosol production by acid-catalyzed particle-phase reactions. Science 298, 814–817.

Kalberer, M., Yu, J., Cocker, D.R., Flagan, R.C., Seinfeld, J.H., 2000. Aerosol formation in the cyclohexene–ozone system. Environmental Science and Technology 34, 4894–4901.

Kamens, R., Jang, M., Chien, C., Leach, K., 1999. Aerosol formation from the reaction of α-pinene and ozone using a gas-phase kinetics-aerosol partitioning model. Environmental Science and Technology 33, 1430–1438.

Kim, Y.P., Seinfeld, J.H., 1995. Atmospheric gas-aerosol equilibrium, III, Thermodynamics of crustal elements Ca^{2+}, K^{+}, and Mg^{2+}. Aerosol Science and Technology 22, 93–110.

Kim, Y.P., Seinfeld, J.H., Saxena, P., 1993a. Atmospheric gas–aerosol equilibrium, I, Thermodynamic model. Aerosol Science and Technology 19, 157–181.

Kim, Y.P., Seinfeld, J.H., Saxena, P., 1993b. Atmospheric gas–aerosol equilibrium, II, analysis of common approximations and activity coefficient calculation methods. Aerosol Science and Technology 19, 182–198.

Kleeman, M.J., Cass, G.R., 1998. Source contributions to the size and composition distribution of urban particulate air pollution. Atmospheric Environment 32, 2803–2816.

Koo, B., Gaydos, T.M., Pandis, S.N., 2003. Evaluation of the equilibrium, dynamic, and hybrid aerosol modeling approaches. Aerosol Science and Technology 37, 53–64.

Lee, S., Kamens, R.M., 2002. The effect of background aerosols on secondary organic aerosol formation: α-pinene and NO_x photo oxidation system. Presented at 21st Annual Conference of American Association for Aerosol Research, Charlotte, NC, US, 7–11 October.

Li, Z., Li, Y., Lu, J., 1999. Surface tension model for concentrated electrolyte aqueous solutions by the Pitzer equation. Industrial and Engineering Chemistry Research 38, 1133–1139.

Meng, Z., Dabdub, D., Seinfeld, J.H., 1998. Size-resolved and chemically resolved model of atmospheric aerosol dynamics. Journal of Geophysical Research 103, 3419–3435.

Ming, Y., Russell, L.M., 2002. Thermodynamic equilibrium of organic-electrolyte mixtures in aerosol particles. AIChE Journal 48, 1331–1348.

Molnár, A., Mészáros, E., Hansson, H.C., Karlsson, H., Gelencsér, A., Kiss, G.Y., Krivácsy, Z., 1999. The importance of organic and elemental carbon in the fine atmospheric aerosol particles. Atmospheric Environment 33, 2745–2750.

Nath, S., 1999. Surface tension of nonideal binary liquid mixtures as a function of composition. Journal of Colloid and Interface Science 209, 116–122.

Nenes, A., Pandis, S.N., Pilinis, C., 1998. ISORROPIA: a new thermodynamic equilibrium model for multiphase multicomponent inorganic aerosols. Aquatic Geochemicals 4, 123–152.

Odum, J.R., Hoffmann, T., Bowman, F., Collins, D., Flagan, R.C., Seinfeld, J.H., 1996. Gas/particle partitioning and secondary organic aerosol yields. Environmental Science and Technology 30, 2580–2585.

Odum, J.R., Jungkamp, T.P.W., Griffin, R.J., Flagan, R.C., Seinfeld, J.H., 1997a. The atmospheric aerosol-forming potential of whole gasoline vapor. Science 276, 96–99.

Odum, J.R., Jungkamp, T.P.W., Griffin, R.J., Forstner, H.J.L., Flagan, R.C., Seinfeld, J.H., 1997b. Aromatics, reformulated gasoline, and atmospheric organic aerosol formation. Environmental Science and Technology 31, 1890–1897.

Pandis, S.N., Harley, R.A., Cass, G.R., Seinfeld, J.H., 1992. Secondary organic aerosol formation and transport. Atmospheric Environment 26A, 2269–2282.

Pandis, S.N., Wexler, A.S., Seinfeld, J.H., 1993. Secondary organic aerosol formation and transport, II, Predicting the ambient secondary organic aerosol size distribution. Atmospheric Environment 27A, 2403–2416.

Pandis, S.N., Wexler, A.S., Seinfeld, J.H., 1995. Dynamics of tropospheric aerosols. Journal of Physical Chemistry 99, 9646–9659.

Pankow, J.F., 1994a. An absorption-model of gas-particle partitioning of organic-compounds in the atmosphere. Atmospheric Environment 28, 185–188.

Pankow, J.F., 1994b. An absorption-model of the gas aerosol partitioning involved in the formation of secondary organic aerosol. Atmospheric Environment 28, 189–193.

Peng, C., Chan, M.N., Chan, C.K., 2001. The hygroscopic properties of dicarboxylic and multifunctional acids: measurements and UNIFAC predictions. Environmental Science and Technology 35, 4495–4501.

Petäjä, T., Aalto, P., Hämeri, K., 2002. Hygroscopicity of toluene oxidation products. Presented at 6th International Aerosol Conference, Taipei, Taiwan, 8–13 September.

Pilinis, C., Seinfeld, J.H., 1987. Continued development of a general equilibrium model for inorganic multicomponent atmospheric aerosols. Atmospheric Environment 32, 2453–2466.

Pilinis, C., Capaldo, K.P., Nenes, A., Pandis, S.N., 2000. MADM-A new multicomponent aerosol dynamics model. Aerosol Science and Technology 32, 482–502.

Pun, B.K., Griffin, R.J., Seigneur, C., Seinfeld, J.H., 2002. Secondary organic aerosol, 2, Thermodynamic model for gas/particle partitioning of molecular constituents. Journal of Geophysical Research 107, 4333, doi:10.1029/2001JD000542.

Saxena, P., Hildemann, L.M., 1997. Water absorption by organics: survey of laboratory evidence and evaluation of UNIFAC for estimating water activity. Environmental Science and Technology 31, 3318–3324.

Saxena, P., Hildemann, L.M., McMurry, P.H., Seinfeld, J.H., 1995. Organics alter hygroscopic behavior of atmospheric particles. Journal of Geophysical Research 100, 18755–18770.

Schell, B., Ackermann, I.J., Hass, H., Binkowski, F.S., Ebel, A., 2001. Modeling the formation of secondary organic aerosol within a comprehensive air quality model system. Journal of Geophysical Research 106, 28275–28293.

Seinfeld, J.H., Pandis, S.N., 1998. Atmospheric Chemistry and Physics: From Air Pollution to Climate Change. Wiley, New York.

Seinfeld, J.H., Erdakos, G.B., Asher, W.E., Pankow, J.F., 2001. Modeling the formation of secondary organic aerosol (SOA), 2, The predicted effects of relative humidity on aerosol formation in the α-pinene-, β-pinene-, sabinene-, Δ^3-carene-, and cyclohexene–ozone systems. Environmental Science and Technology 35, 1806–1817.

Sheehan, P.E., Bowman, F.M., 2001. Estimated effects of temperature on secondary organic aerosol concentrations. Environmental Science and Technology 35, 2129–2135.

Stephanou, E.G., Stratigakis, N., 1993. Oxocarboxylic and α,ω-dicarboxylic acids: photooxidation products of biogenic unsaturated fatty acids present in urban aerosols. Environmental Science and Technology 27, 1403–1407.

Stokes, R.H., Robinson, R.A., 1966. Interactions in aqueous nonelectrolyte solutions, I, Solute–solvent equilibria. Journal of Physical Chemistry 70, 2126–2130.

Strader, R., Lurmann, F., Pandis, S.N., 1999. Evaluation of secondary organic aerosol formation in winter. Atmospheric Environment 33, 4849–4863.

Tao, Y., McMurry, P.H., 1989. Vapor pressures and surface free energies of C14–C18 monocarboxylic acids and C5 and C6 dicarboxylic acids. Environmental Science and Technology 23, 1519–1523.

Turpin, B.J., Huntzicker, J.J., 1991. Secondary formation of organic aerosol in the Los Angeles basin: a descriptive analysis of organic and elemental carbon concentrations. Atmospheric Environment 25A, 207–215.

Wexler, A.S., Seinfeld, J.H., 1990. The distribution of ammonium salts among a size and composition dispersed aerosol. Atmospheric Environment 24A, 1231–1246.

Wexler, A.S., Seinfeld, J.H., 1991. Second-generation inorganic aerosol model. Atmospheric Environment 25A, 2731–2748.

Yokouchi, Y., Ambe, Y., 1986. Characterization of polar organics in airborne particulate matter. Atmospheric Environment 20, 1727–1734.

Yu, J., Cocker, D.R., Griffin, R.J., Flagan, R.C., Seinfeld, J.H., 1999. Gas-phase ozone oxidation of monoterpenes: gaseous and particulate products. Journal of Atmospheric Chemistry 34, 207–258.

Zhang, X.Q., McMurry, P.H., Hering, S.V., Casuccio, G.S., 1993. Mixing characteristics and water content of submicron aerosols measured in Los Angeles and at the Grand Canyon. Atmospheric Environment 27A, 1593–1607.